A Deployable Robot Based on the Bricard Linkage

Chapter · November 2016

DOI: 10.1007/978-981-10-2875-5_61

4 authors, including:

Hao Shang
Tianjin University
2 PUBLICATIONS **17** CITATIONS
SEE PROFILE

Dawei Wei
Tianjin University
2 PUBLICATIONS **17** CITATIONS
SEE PROFILE

Rongjie Kang
Tianjin University
71 PUBLICATIONS **1,471** CITATIONS
SEE PROFILE

A Deployable Robot Based on the Bricard Linkage

Hao Shang[1,2], Dawei Wei[1,2], Rongjie Kang[1,2,*] and Yan Chen[1,2] ,

[1] Key Laboratory of Mechanism Theory and Equipment Design of Ministry of Education,
Tianjin University, Tianjin 300072, China
[2] School of Mechanical Engineering,
Tianjin University,Tianjin 300072,China
{shanghao, wdw03, rjkang, yan_chen}@tju.edu.cn

Abstract. A large variety of transformable robots were proposed in the past decades, which were mainly based on reconfigurable mechanisms. Meanwhile, deployable structures have been extensively applied to various fields, such as aerospace industry, civil engineering, and medical engineering. This paper presents a new method to integrate deployable structures to the design of transformable robots. A threefold-symmetric Bricard linkage is analyzed and used as the body structure of the robot. Gait control is then achieved by using the deploying and folding motion of the Bricard linkage. Experimental results show that the robot is capable of moving through limited space with single degree-of-freedom (DOF).

Keywords: threefold-symmetric Bricard linkage, deployable robot, gait control

1 Introduction

In recent years, there has been a growing interest in the development of transformable robots, which can adjust their configurations to adapt to multiple tasks and uncertain environment. Such robots have been widely applied to areas such as reconnaissance, rescue missions, and space applications [1].

Reconfigurable robots are a kind of transformable robots built from modules that can be connected in different ways to form different morphologies for different purposes [3]. Since the Reconfigurable Modular Manipulator System (RMMS) was invented the in 1988 [2], many kinds of reconfigurable robots appeared successively.

Chain-type reconfigurable robots were a typical class of reconfigurable robots, such as the PolyPod robot [4] and later its descendent PolyBot [5] and CONRO [6] shown in Fig. 1 (a).

Another class of reconfigurable robots is the lattice-type robots. Early two-dimensional lattice-type robots include the Fracta and Metamorphic robots [7, 8]; the first three-dimensional lattice-type robots were the Molecule shown in Fig. 1 (b) and the 3-D-Unit [9, 10].

* Corresponding author.
E-mail address: rjkang@tju.edu.cn (R. Kang).

Chain-type and lattice-type robots have evolved to the hybrid reconfigurable robots. The recent generation of self-reconfigurable robots, including M-TRAN III, ATRON shown in Fig.1 (c), and SuperBot, are all of the hybrid type [11, 12, and 13].

In the last decade, a new kind of transformable robots based on metamorphic mechanisms was presented. Dai [14] proposed the concept of metamorphic palm. As shown in Fig.1 (d), a robotic hand in which the palm section enables it to achieve a wide range of movement was designed. Ding [15, 16] proposed a novel design of metamorphic hybrid wheel-legged rover mechanism.

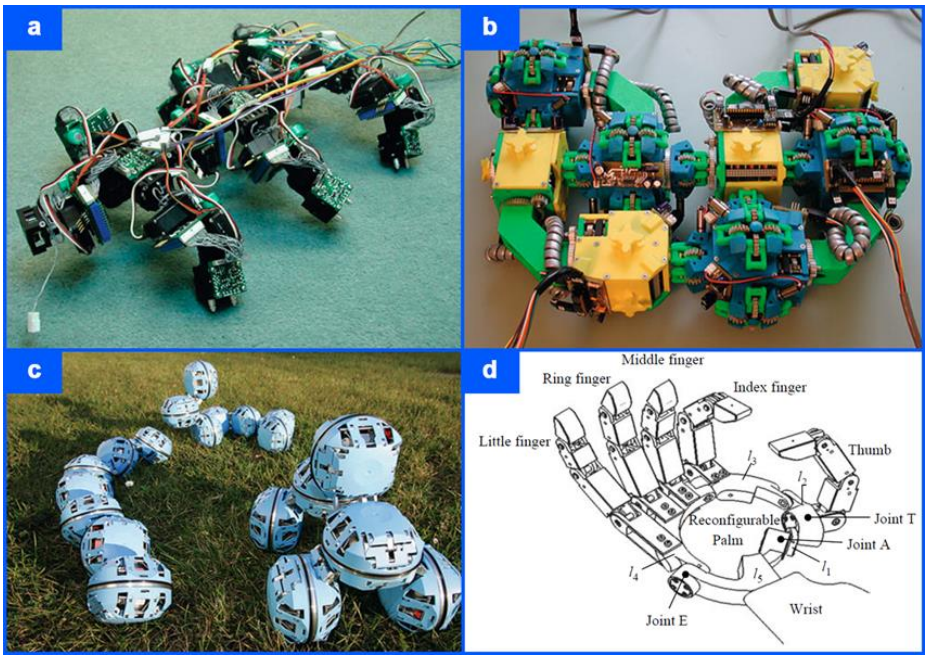

Fig.1. Transformable robot
(a) CONRO (b) Molecule
(c) ATRON (d) metamorphic palm

However, the above-mentioned robots are not able to change their size significantly, which is important for passing through constrained environment.

Meanwhile, since the first overconstrained mechanism was proposed by Sarrus [17], a number of overconstrained mechanisms have been proposed by some researchers including Bennett in 1903 [18, 19], Bricard in 1926 [20], Myard in 1931 [21], Goldberg in 1943 [22], Waldron in 1968 [23], and Wohlhart in 1987 [24]. After that the overconstrained mechanisms, especially Bennett and Bricard linkages, were applied to deployable structures by Chen [25, 26, and 27]. A large variety of deployable structures were used in engineering fields. Catherine used the Hoberman

mechanism to design reconfigurable antenna and solar arrays [28]. Wohlhart also developed a deployable polyhedron by using a set of planar linkages [29]. Gantes [30], Hanaor [31] and Pellegrino [32] et al. applied to the civil engineering structures.

Although deployable structures have achieved great progress in the fields of aerospace industry, civil engineering, and medical engineering, there were seldom applications in the design of transformable robots.

The aim of this paper is to use the deployable structure to develop a novel transformable robot. The threefold-symmetric Bricard linkage is adopted here due to its large expansion ratio and single DOF moving ability that allows for easy control. The presented robot can change its configuration to go through a narrow gap either perpendicular or parallel to the ground.

The paper is organized as follows. Section 2 shows the analysis of geometrical properties of the threefold-symmetric Bricard linkage. Section 3 presents the design of the robot including the mechanism analysis, gaits generation and control system. Section 4 presents the experimental results, and Section 5 gives the conclusion and discussion.

2 Bricard Linkage

The Bricard linkage is the only 6R overconstrained linkage independent from other linkages. There are six distinct types of Bricard linkages in the family of Bricard linkage. They were discovered and reported by Bricard [33]. In 2005, Chen et al.[34] presented a kinematic analysis of a new linkage called *Threefold-symmetric Bricard linkage*, which was obtained by combining the general plane-symmetric and trihedral Bricard linkage, and pointed out the possibility of applying this linkage to deployable structures.

The configuration of this linkage is shown in Fig. 2. It has three symmetric planes and threefold-rotational symmetry. Each link of the linkage is perpendicular to the two axes of adjacent revolute joints it connects.

The threefold-symmetric Bricard linkage satisfies the following conditions:

$$\begin{cases} a_{12}=a_{23}=a_{34}=a_{45}=a_{56}=a_{61}=l, \\ \alpha_{12}=\alpha_{34}=\alpha_{56}=\alpha, \quad \alpha_{23}=\alpha_{45}=\alpha_{61}=2\pi-\alpha, \\ R_i=0 (i=1,2,3,4,5,6) \\ \theta_1=\theta_3=\theta_5=\theta \\ \theta_2=\theta_4=\theta_6=\varphi \end{cases} \tag{1}$$

where a_{jk} is the length of a link between two adjacent axes of revolute j and k, α_{jk} is the twist angle between axes of adjacent revolute joints j and k (j, k=1, 2, 3, 4, 5, 6), and R_i is the offset between endpoints of two links connected by one revolute joint along the axis i. θ_i is the rotation angle about axis of joint i.

The closure equation of this threefold-symmetric linkage is then obtained by

$$\cos^2\alpha+\sin^2\alpha(\cos\theta+\cos\varphi)+(1+\cos^2\alpha)\cos\theta\cos\varphi-2\cos\alpha\sin\theta\sin\varphi=0 \tag{2}$$

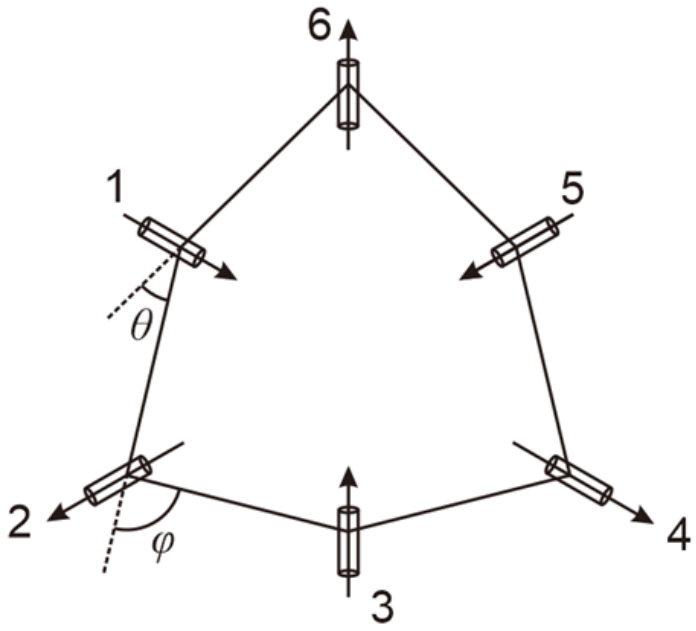

Fig.2. Threefold-symmetric Bricard linkage

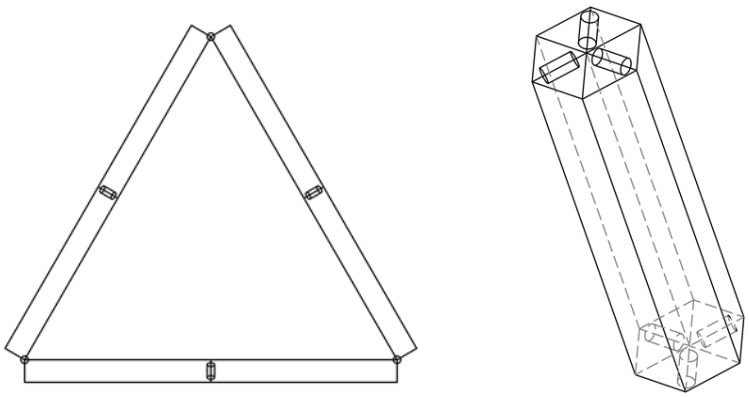

(a) (b)

Fig.3. The structure which is applied to the robot
(a) The deployed configuration;
(b) The folded configuration.

The structure when $l = 500mm, \alpha = 2\pi/3$ as shown in Fig.3 is chosen to build the model of the deployable robot.

The reasons for selecting these parameters can be listed as follows:

1. For $0 \le \alpha < \pi/3$, or $2\pi/3 < \alpha \le \pi$, the movement of linkages is not continuous. Thus, the linkage is physically blocked in the positions where all links crossed at the center when either θ or φ reaches π or $-\pi$. When $\pi/3 \le \alpha \le 2\pi/3$, the linkage keeps moving continuously [34].

2. When $\alpha = \pi/3$ or $\alpha = 2\pi/3$, the movement of the linkages has a kinematic bifurcation, which means the number of instantaneous (infinitesimal) degrees of freedom increases. Although we took some measures to avoid this robot movement curve pass the bifurcation point in this paper. By taking advantage of kinematic bifurcation, there is an infinite possibility with the future to develop the robot that will have more ways in transformation.

3. In fact, for $\alpha = \pi/3$ and $\alpha = 2\pi/3$, the linkages have the same kinematic properties. So we had chosen one of it.

4. To adapt to the size of other parts that assembled the robot, $l = 500mm$ was selected.

Substituting $\alpha = 2\pi/3$ into equation (**2**), we can reach the input–output equation:

$$\frac{1}{4} + \frac{3}{4}(\cos\theta + \cos\varphi) + \frac{5}{4}\cos\theta\cos\varphi + \sin\theta\sin\varphi = 0 \tag{3}$$

Figure 4 shows the input–output curve (green color) determined by equation (**3**). According to Figures 3 and 4, the properties for the threefold-symmetric linkage when $\alpha = 2\pi/3$ are as follows. Firstly, it appears that only one of the six revolute variables can be free. Thus, this threefold-symmetric linkage has one degree of finite mobility. Secondly, it can be flattened to form a planar equilateral triangle with side length $2l$. Additionally, the linkage keeps moving continuously.

However, as shown in Fig.4, the point at $(\theta, \varphi) = (\pi, \pi)$ is the point of bifurcation. This means the linkage has 2 DOF in this point, which causes the unexpected motion. Meanwhile, when $(\theta, \varphi) = (0, 2\pi/3)$, the linkage is in the deployed configuration. It's difficult to change the linkage structure to the folded configuration because of the overload torque. So as shown in Fig.4, the curve in red color, in which θ varies from $\pi/10$ to $9\pi/10$, is used for the robot to perform walking motions.

The reasons for applying this linkage for the robot are that the linkage has single DOF and simple structure, which make the actuation and control easy and feasible. Moreover, the linkage has a large expansion ratio, meaning that it can change its size significantly.

3 Design of the Deployable Robot

Based on the above analysis this section presents the design of the deployable robot using the threefold-symmetric Bricard linkage. In the first part, the mechanical design

of the robot is elaborated in detail. Two gaits of the robot are presented in the second part. The final part discusses a double closed loop control system applied to the robot.

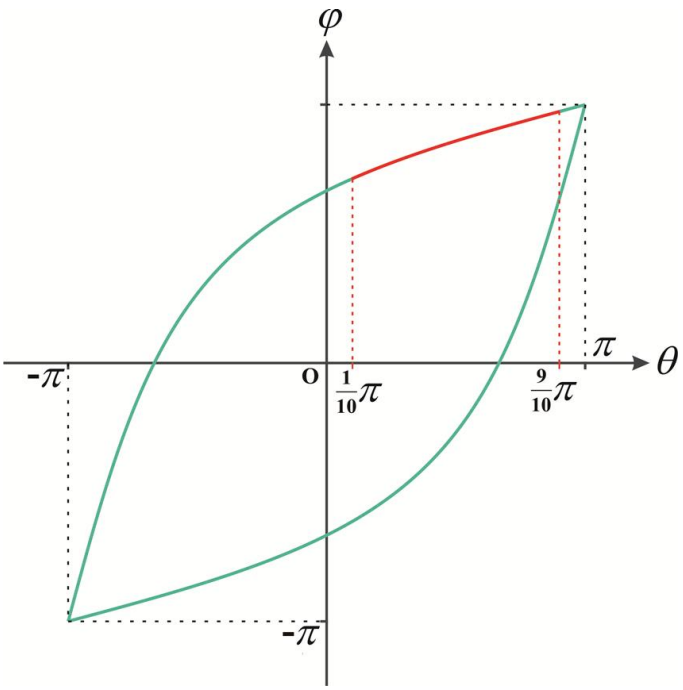

Fig.4. θ versus φ for the threefold-symmetric linkage for $\alpha = 2\pi/3$

3.1 The Mechanical Design

To build a lightweight, flexible and high strength deployable robot, carbon fiber tubes are used to form the robot body. The "feet", constituted with steel frame and wheels, play a significant role in supporting the body, walking and transforming. The transmission gears, battery and the DC-motor are located inside the steel frame. Meanwhile, the angle sensor is assembled collinearly with the joint axis to monitor the rotation angle θ, which is the parameter of the linkage as shown in Fig.2, and the control module (CMOD) is fixed on the robot body. In addition, Omni-directional wheels are used to achieve a batter gait. The robotic prototype is shown in Fig. 5.

The area of the robot can reach 0.027 m^2 in minimum and 0.73 m^2 in maximum with the height of 0.68 m and 0.2 m. In deployed form, θ is set $\pi/10$ to facilitate folding. Meanwhile the maximum of θ is $9\pi/10$ to avoid bifurcation in folded form. It has a good transformation property with expansion ratio of 27.04 (defined as ratio of bottom area of the deployed and folded form).

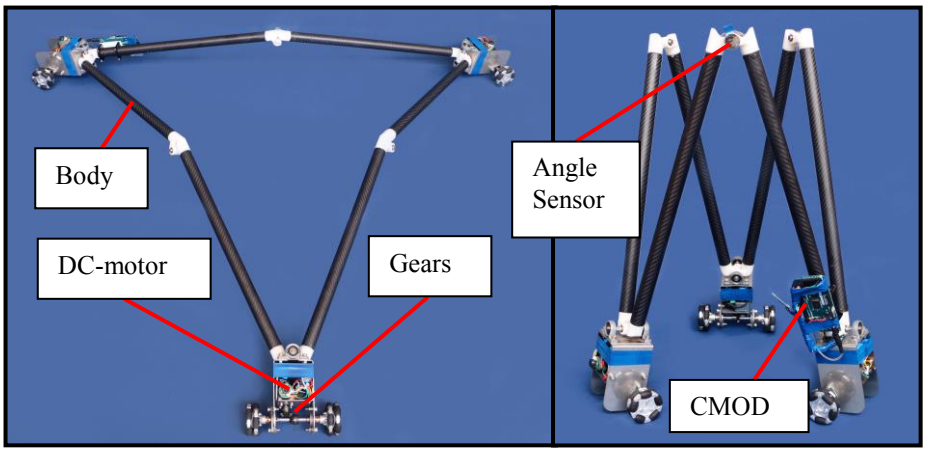

(a) (b)

Fig.5. The robotic prototype
(a) The deployed configuration; (b) The folded configuration.

3.2 Gait of the Robot

The robot is actuated by three DC-motors, while it has single DOF. We designed two kinds of gaits to achieve walking.

One is simply to change the configuration of the robot's body, called deployed-folded gait. As the structure has good symmetry and single DOF, the deployed-folded gait is performed by activating the three motors at the same time with identical rotating speed. As shown in Fig.6 (a), in the deployed configuration, the three feet move outward synchronously to the deployed form. In the folded configuration they move inversely to the folded form. In this gait the robot will not walk but change its size and height.

The other gait is designed for the robot to walk in a specific direction, called directional gait. In this gait one motor is locked and the others are activated in sequence at identical rotating speed. So that the robot moves forward.

As shown in Fig.6 (b), at the beginning, the foot 2 is locked while the feet 1 and 3 moves outward. The centroid of the robot moves from the point s1 to s2. Then the foot 2 and foot 3 move inward while the foot 1 is locked, and the centroid of the robot moves from the point s2 to s3. Afterwards the robot deploys with the foot 3 locked, and the robot moves from s3 to s4. Finally, the robot folds with the foot 1 locked, and moves from s4 to s5. During a circle of all steps, the robot completes a forward motion from s1 to s5.

In the directional gait, the motors are not allowed for delay to ensure synchronization. Therefore, a self-locking motor is selected. Meanwhile, the composite force of the working feet exerted by the robot body is not parallel to the motion of the wheels. Therefore, there exists a friction perpendicular to the movement of the feet. Omni-directional wheels are employed in case of lateral slip.

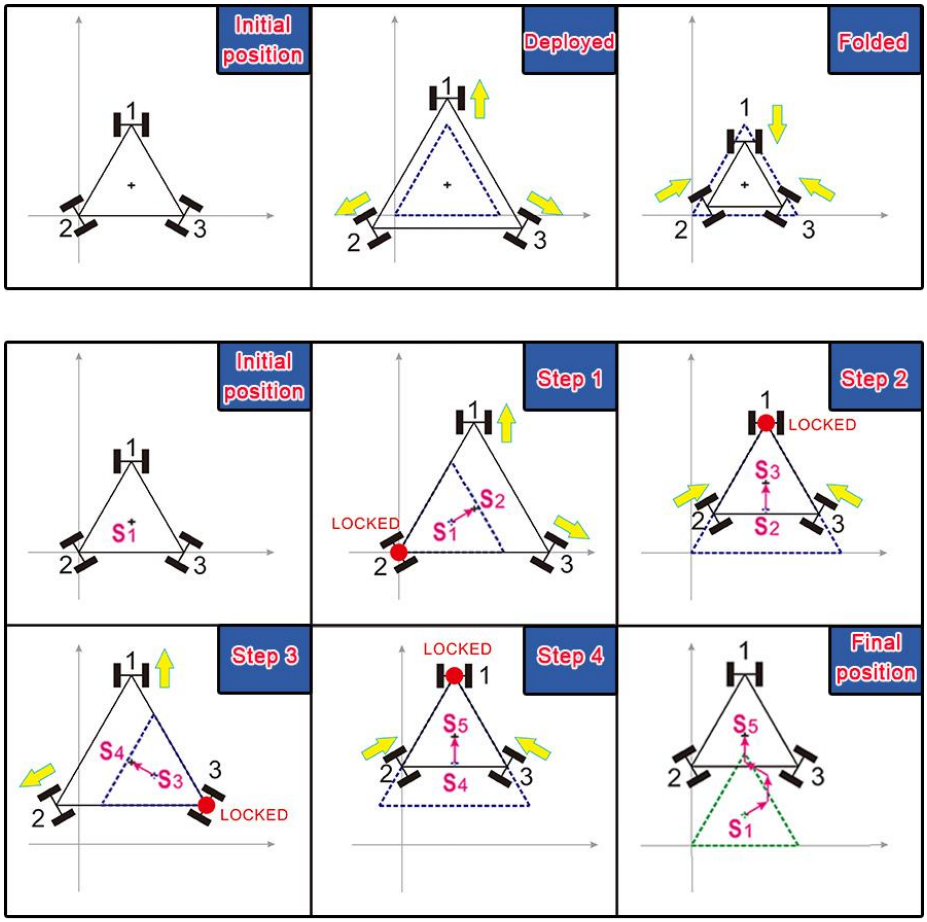

Fig.6. The forward gait
(a) The deployed-folded gait
(b) The directional gait

3.3 The Control System Design

The robotic control system consists of a host computer, an on-board micro-computer (Arduino Mega 2560), three DC motors with transmission system, three electromagnetic encoders on the motors, and an angle sensor on one joint of the linkage, Fig.5(b).

Control commands, like walking direction and speed, are sent by the host computer and received by the on-board micro-computer via a Bluetooth module. The micro-computer then converts the control commands to level signals and PWM signals to drive the three motors. The rotating speed of the motors are fed back to the micro-computer to form a velocity control loop with a PID algorithm while the angle θ is fed back to the micro-computer form a position control loop. The angle θ is also sent back to the host computer to show the position of the robot to the operator.

4 Experiment

In order to illustrate the performance of the robot, two experiments were conducted. One is to test the deploying motion of the robot, in which the rotation angle θ increases from 43° to 77°. As shown in Fig.7, the rotation angle θ goes up with a constant rate after 0.3 seconds. This indicates that the motion of the robot reaches stability in a short time, which reflects a good control performance.

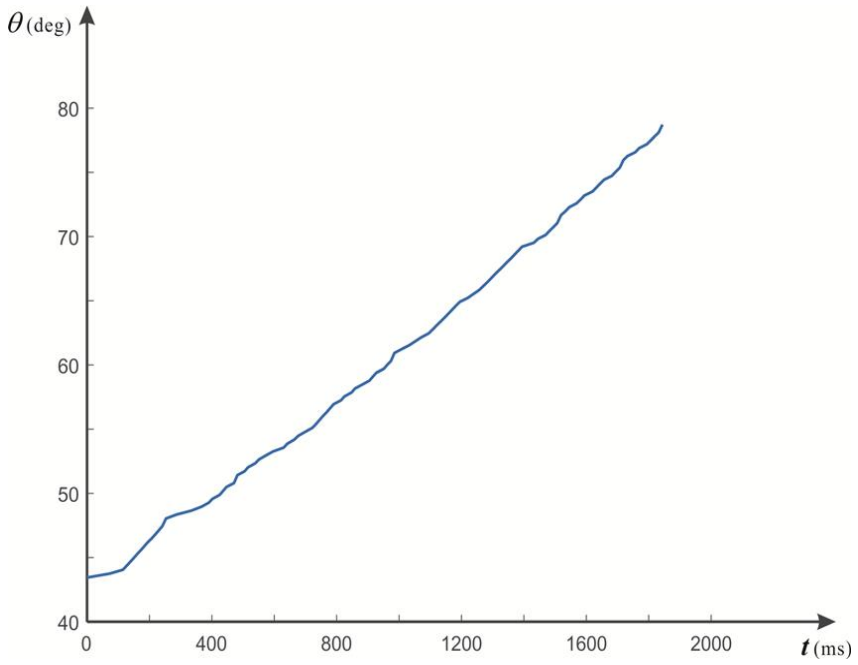

Fig.7. θ versus t in the folding process

The second experiment is to test the ability of the robot to pass narrow gaps. Two kinds of circumscribed paths are established as shown in Fig.8. The first, in Fig.8 (a), is a 400 mm high gap. The robot deploys to a position where θ reaches 150 degrees and then advances in the directional gait during which the height varies from 0.2 m to

0.3 m. To pass through the second path shown in Fig.8 (b) whose width is 600 mm, the robot folds to an extent that θ is 30 degrees and keeps moving in the directional gait with its width fluctuating from 0.4 m to 0.5 m. The experiment demonstrates high adaptability of the robot to variable and limited space.

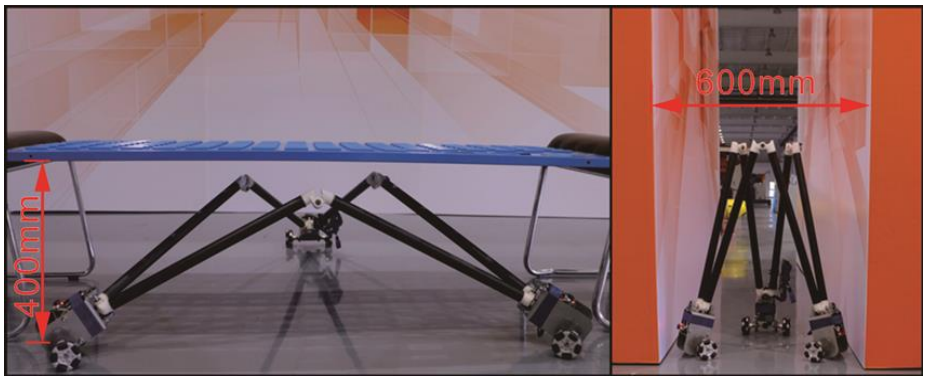

(a) (b)

Fig.8. Field condition of the passing experiment
(a) A horizontal gap; (b) A vertical gap

5 Conclusion and Discussion

In this paper, a new deployable robot based on threefold-symmetrical Bricard linkage is proposed. It is a single-DOF robot with unique gaits achieved by the deploying and folding movements of the structure. DC motors are utilized to actuate the robot. A rotating speed-angle double loop control system is applied to the robot to improve control performance. The robot exhibits good adaptively when passing through limited space.

Future work will focus on exploring other forms of Bricard linkages applicable to deployable robots, which can fulfill tasks like stair climbing, and focus on its control stability.

References

1. Salemi, B., Moll, M., Shen, W.M.: SUPERBOT: A deployable, multi-functional, and modular self-reconfigurable robotic system, pp. 3636--3641. IEEE International Conference on Intelligent Robots and Systems (2006)
2. Schmitz, D., Khosla, P., Kanade, T.: The CMU Reconfigurable Modular Manipulator System. Technical Report (1988)
3. Støy, K.: Reconfigurable Robots. Springer Berlin Heidelberg (2015)
4. Yim, M.: Locomotion With A Unit-Modular Reconfigurable Robot. Stanford University (1998)
5. Duff, D.G., Yim, M., Roufas, K.: Evolution of PolyBot: A Modular Reconfigurable Robot. Proc of the Harmonic Drive International Symposium (2001)
6. Castano, A., Ramesh, Chokkalingam, Will, P.: Autonomous and Self-Sufficient CONRO Modules for Reconfigurable Robots. International Symposium on Distributed Autonomous Robotic Systems (2000)
7. Murata, S., Kurokawa, H., Kokaji, S.: Self-assembling machine. IEEE International Conference on Robotics and Automation. Proceedings, pp. 441--448 (1994)
8. Chirikjian, G.S.: Kinematics of a metamorphic robotic system. IEEE International Conference on Robotics and Automation. pp. 449--455 (1994)
9. Kotay, K., Rus, D., Vona, M., Mcgray, C.: The self-reconfiguring robotic molecule. IEEE International Conference on Robotics and Automation, pp. 424--431 (1998)
10. Murata, S., Kurokawa, H., Yoshida, E., Tomita, K.: A 3-D self-reconfigurable structure. IEEE International Conference on Robotics and Automation, pp. 432—439 (1998)
11. Salemi, B., Moll, M., Shen, W.M.: SUPERBOT: A Deployable, Multi-Functional, and Modular Self-Reconfigurable Robotic System. IEEE International Conference on Intelligent Robots and Systems, pp. 3636--3641 (2006)
12. Kurokawa, H., Tomita, K., Kamimura, A., Kokaji, S., Hasuo, T.: Distributed self-reconfiguration of M-TRAN III modular robotic system. International Journal of Robotics Research, 27(3-4), pp. 373--386 (2008)
13. Stergaard, E.H., Kassow, K., Beck, R., Lund, H.H.: Design of the ATRON lattice-based self-reconfigurable robot. Autonomous Robots, 21(2), pp. 165--183 (2006).
14. Wei, G., Dai, J.S., Wang, S., Luo, H.: Kinematic Analysis and Prototype of a Metamorphic Anthropomorphic Hand with a Reconfigurable Palm. International Journal of Humanoid Robotics, 8(3), pp. 459--479 (2011)
15. Wang, Z., Ding, X., Rovetta, A.: Structure design and locomotion analysis of a novel robot for lunar exploration. Iftomm World Congress (2007)
16. Ding, X.L., Kun, X.U.: Design and analysis of a novel metamorphic wheel-legged rover mechanism. Zhongnan Daxue Xuebao, 40, pp. 91--101 (2009)
17. Sarrus P T, C.: Note sur la transformation des mouvements rectilignes alternatifs, en mouvements circulaires; et reciproquement. Academie des sciences. pp. 1036--1038 (1853)
18. Bennett, G.T.: A new mechanism. Engineering (76), pp. 777--778 (1903)
19. Bennett, G.T.: The Skew Isogram Mechanism. Proceedings of the London Mathematical Society, 13(1), pp. 151--173 (1914)
20. Bricard, R.: Le çons de cin ématique: Gauthier-Villars (1926)
21. Myard, F.E.: Contribution à la g éom étrie des syst èmes articul és. Bull.soc.

math.france, 59, pp. 183--210 (1931)
22. Goldberg, M., Goldberg, M.: New five-bar and six-bar linkages in three dimensions. Transactions of the Asme (1943)
23. Waldron, K.J.: Hybrid overconstrained linkages. Journal of Mechanisms, 3(2), pp. 73--78 (1968)
24. Wohlhart, K.: A new 6R space mechanism. Proceedings of the Seventh World Congress on the Theory of Machines and Mechanisms, Sevilla, Spain, pp. 193--198 (1987)
25. Chen, Y., You, Z.: Square Deployable Frames for Space Applications. Part 1: Theory. Proceedings of the Institution of Mechanical Engineers Part G Journal of Aerospace Engineering, 220(4), pp. 347--354 (2006)
26. Chen, Y., You, Z.: Square deployable frames for space applications. Part 2: Realization. Proceedings of the Institution of Mechanical Engineers Part G Journal of Aerospace Engineering, 221(1), pp. 37--845 (2007)
27. Chen, Y., You, Z.: Curved-profile deployable structures based on Bennett linkages. Aiaa/asme/asce/ahs/asc Structures, Structural Dynamics, and Materials Conference (2007)
28. Faist, K.A., Wiens, G.J.: Parametric study on the use of Hoberman mechanisms for reconfigurable antenna and solar arrays. Aerospace Conference, 2010 IEEE, pp. 1--8 (2010)
29. Wohlhart, K.: Polyhedral Zig-Zag Linkages. Springer Netherlands. (2004)
30. Gantes, C.J., Connor, J.J., Logcher, R.D., Rosenfeld, Y.: Structural analysis and design of deployable structures. Computers & Structures, 32(3-4), pp. 661--669 (1989)
31. Hanaor, A., Levy, R.: Evaluation of Deployable Structures for Space Enclosures. International Journal of Space Structures, 16(4), pp. 211--229 (2001)
32. Pellegrino, S.: Deployable Structures in Engineering. Deployable Structures (2001)
33. R. Bricard, Mémoire sur la théorie de l'octaèdre articulé, J. Math. Pures Appl. 3(5), pp. 11--148 (1897)
34. Chen, Y., You, Z., Tarnai, T.: Threefold-symmetric Bricard linkages for deployable structures. International Journal of Solids & Structures, 42(8), pp. 2287--2301 (2005)